



Shahid Bahonar University of  
Kerman



**Biomechanism and Bioenergy Research**

Online ISSN: 2821-1855  
Homepage: <https://bbr.uk.ac.ir>



Iranian Society of Agricultural Machinery  
Engineering and Mechanization

## A Dynamic Model for Estimating Tire Contact Patch Using Machine Vision Techniques

Sajjad Derafshpour<sup>1</sup>, Aref Mardani<sup>1</sup>, Morteza Valizadeh<sup>2</sup>

<sup>1</sup> Department of Mechanical Engineering of Biosystems, Urmia university, Urmia, Iran.

<sup>2</sup> Department of Electrical Engineering, Urmia University, Urmia, Iran.

 Corresponding author: [a.mardani@urmia.ac.ir](mailto:a.mardani@urmia.ac.ir)

### ARTICLE INFO

**Article type:**

Research Article

**Article history:**

Received 12 October 2023

Received in revised form 05  
November 2023

Accepted 18 December 2023

Available Online 28 December  
2023

**Keywords:**

Contact patch, Bat algorithm,  
Image processing technique,  
Metal box.

### ABSTRACT

Tire is the main connection between a vehicle and the road that significantly affects the dynamic behavior and the performance of it. Tires also influence other characteristics of vehicles such comprising fuel consumption, handling, ride quality, traction, braking performance and stability. The importance of investigating the contact patch is valuable from perspective of increasing traction efficiency to reducing fuel consumption. In this research, the contact patch of the wheel was investigated based on experimental-analytical methods. The dynamically contact tire patch was utilized using an image processing technique. Then, contact patch was modeled by the Bat algorithm considering the load on the tire and inflation pressure. Evaluation of the model revealed that error rate compared with observed data (extracted from image processing) is equal to 4%. The calculated coefficient of determination ( $R^2$ ) for this model was 95% which indicates the high credibility of the model for dynamic conditions.

**Cite this article:** Derafshpour, S., Mardani, A., & Farzaneh B (2023). A Dynamic Model for Estimating Tire Contact Patch Using Machine Vision Techniques. *Biomechanism and Bioenergy Research*, 2(2), 28-38. <https://doi.org/10.22103/BBR.2023.22328.1056>



© The Author(s).

DOI: <https://doi.org/10.22103/BBR.2023.22328.1056>

**Publisher:** Shahid Bahonar University of Kerman

## INTRODUCTION

Tire is considered as the only connection between automotive and road. The dynamic behavior and the performance of the vehicle is affected by this component. Moreover, tire influences other characteristics of the vehicle comprising fuel consumption, handling, ride quality, traction, braking performance, stability, etc. (Kusaka & Suzuki, 2013). Another key point to note here is that tire supports all of the external forces applied to the vehicle (i.e., vertical load, longitudinal forces and lateral forces) with the exception of the aerodynamics forces. These forces are brought into being in tire-road interaction area which is known contact patch. Since contact patches can be considered as determining factor in operation condition, a comprehensive investigation of that seems significant. More the point, by analyzing the contact patch, further information can be revealed in vehicle dynamic domain comprising contact features (e.g., shape, size, pressure distribution, shear stresses,), tribology, vehicle safety, slip ratio, etc. For example, analysis and estimation of the energy loss in tire deformation process strongly depends on the contact patch determination. The energy loss at the contact length can be expressed in accordance with Eq (1).

$$E = F.W.L \quad (1)$$

Where  $F$  is the rolling resistance coefficient,  $W$  is the load on the wheel and  $L$  is the contact length. The most obvious being that determination of contact patch in dynamic condition is important not only in tire design but also in computation of required energy for tire deformation. To fulfil this dire need, an efficient model must be developed that can estimate the contact patch as a function of load and inflation pressure. This model can be utilized in vehicle dynamic simulation and its control (Zhang et al., 2013).

Researches into contact patch models are categorized from developing the analytical models, which are based on the applying of the finite element models, boundary area or family of

brush (Ivanov & Augsburg, 2008), to empirical types. Numerous types of analytical models have been proposed in the recent years to evaluate the performance of the tire. The nature of the models is usually accompanied by complex descriptions of interaction due to shell-like structure of tire. In contrast, models derived from experimental data are employed to determine the role of each parameter affecting vehicle performance (Gillespie, 2021).

The basic assumption in the calculation of contact patch is that the tire-road footprint is closer to rectangular or an elliptic shape (Minca, 2015; Redrouthu & Das, 2014; Rill, 2019; Sreekumaran & Iqbal, 2019).

Godbole, Alcock, & Hettiaratchi (1993), based this assumption, suggested models for rectangular and elliptic shape of the contact patch in terms of the tire diameter, the tire section height and tire deflection. However, estimation of the tire deflection in dynamic behavior can be considered difficult. Despite the simplicity of this method, the static approach used in this method can be regarded as its disadvantage. Researches have made multiple attempts to calculate the contact patch dynamically and they have reported various techniques for measuring it. The use of sensor equipment is one of them (Els et al., 2016). As an example of this category, Braghin et al (2006) utilized accelerometers putting inside the tire in order to determine the contact forces and patches features. They calculated contact force by applying the difference between the minimum and maximum value at the point of the exit of the contact patch. However, there was no mention to the contact patch value. The use of image processing techniques as powerful instruments is common in measuring this parameter. In this method, tire moves on a rigid glass. The glass surface is covered with colored material and a digital camera located under the glass surface, which takes video while the tire is passing over it (Abdi-pour & Shamsi, 2023; Derafshpour et al., 2019). Meanwhile, contact patch measurement analysis is carried out by segmentation of the taken images into touching and non-touching area. Therefore, this strategy can be high

precision and accurate alongside dynamic measurement.

This research focuses on developing a new empirical model for estimation of the contact patch. Contact patch is affected by many factors comprising load, inflation pressure, slip, forward velocity, etc. The load on the tire and tire inflation pressure are considered as distinguished factors on the contact patch change. The model was established as a function of load on the tire and tire inflation pressure, which can perform in dynamic condition. In this research, first the contact patch was measured by image processing setup and then using the measured contact patch and test parameters a closed form model was introduced by employing Bat optimization algorithm.

## MATERIALS AND METHODS

This part falls into four sections comprising (1) single wheel tester and data acquisition setup, (2) glass box fabrication, (3) applying the image processing technique for evaluation of contact patch, (4) providing a mathematical model for estimation of contact patch based on evolutionary algorithm.

### Single wheel tester (SWT)

Data acquisition process was performed in soil bin of Terramechanics laboratory. This system was equipped a single wheel tester which is connected to the carriage through an L-shape frame. The carriage was powered by endless chains connected to the 22 kW electromotor. The connection of the tester hub to L-shape frame and carriage was provided by the four-bar mechanism. In order to measure tire rolling resistance, four Bongshin load cells after calibration were placed between the carriage and hub tester on four parallel arms horizontally. Wheel tester speed changing as well as the reverse movement was performed by using an inverter. Load cells connected to a 10-channels data logger and data were recorded and saved by USB port in real-time. The utilized tire was a standard tire (Michelin brand) with the 185/65 R14 86 H specifications. The details of this setup have been described in (Derafshpour et al., 2020). The general shape of the experimental data acquisition setup is observed in Fig 1.

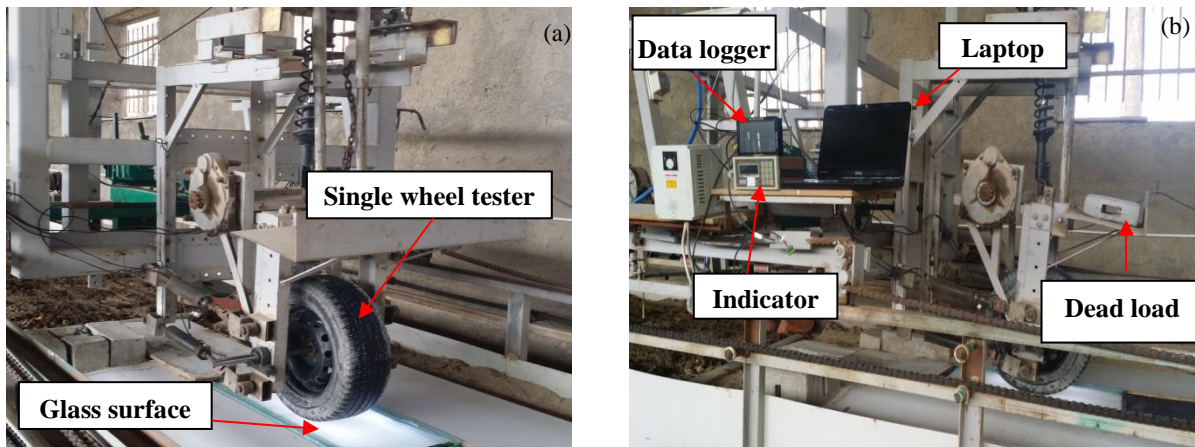


Fig 1. Single wheel tester and data acquisition systems: a) Interaction between tire and glass surface; b) Data acquisition setup

### Glass box fabrication for contact length measurement

An ingenious remedy was employed to observe the amount of this quantity in real-time. For this

purpose, a metal box was fabricated with a dimension of 130 cm in length, 40 cm in width and 50 cm in depth. This box was buried in the soil channel. The surface of the box was covered with safety glass with 20 mm thickness (Fig 2).

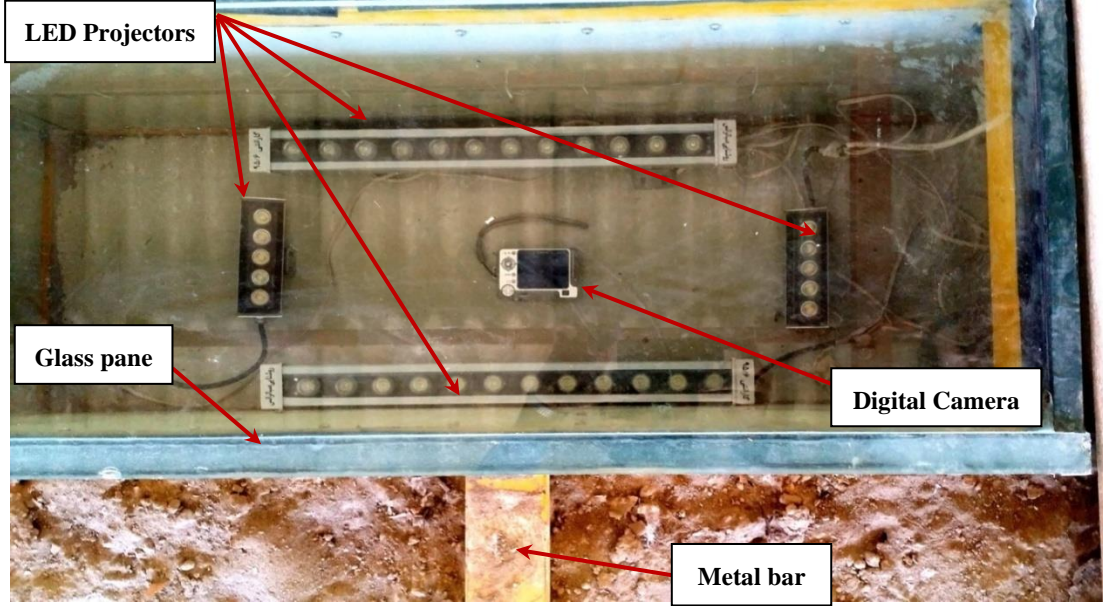


Fig 2. Glass box image capturing pieces of equipment

### Image processing implement for data analysis

The presented metal box is employed for contact patch measurement. A white liquid is poured on the glass and the camera, placed in the metal box, captures a video film whilst the tire passes over the glass. The frames of the video are analyzed to extract the contact patch. Fig 4 shows a sample frame of the video, in which the contact patch can be easily distinguished. The region of glass which touches the tire is seen in black and other regions are seen in gray color. To automatically separate the touching and non-touching regions, appropriate preprocessing and thresholding methods are employed. The preprocessing step subtracts the first frame of the video, representing an estimation of the background, from the current frame according to Eq (2), to generate the difference image that is defined to facilitate the separation of touching and non-touching pixels.

$$D_k = |I_k - I_0| \quad (2)$$

Where  $I_k$  is an image representing the k-th frame of the video and  $D_k$  is its corresponding difference image.

The difference image is binarized using the following equation.

$$B_k(x, y) = \begin{cases} 1 & D_k(x, y) \geq T_k \\ 0 & D_k(x, y) < T_k \end{cases} \quad (3)$$

Where 0 and 1 values represent the touching and non-touching pixels, respectively and  $T_k$  is a threshold obtained according to Eq (4).

$$T_k = \max(75, T_{otsu}) \quad (4)$$

$T_{otsu}$  denotes the threshold of Otsu's method calculated on  $D_k$ . More details about touching and non-touching pixels classification can be found in our previous work (Derafshpour et al., 2019). After binarization of difference image, the image B is processed by opening morphological filter to eliminate those pixels erroneously classified as touching pixels, also an appropriate closing morphological filter is used to fill the holes appeared in touching regions because of LED light reflection and tire tread. Fig 3 shows the result of contact area extraction.

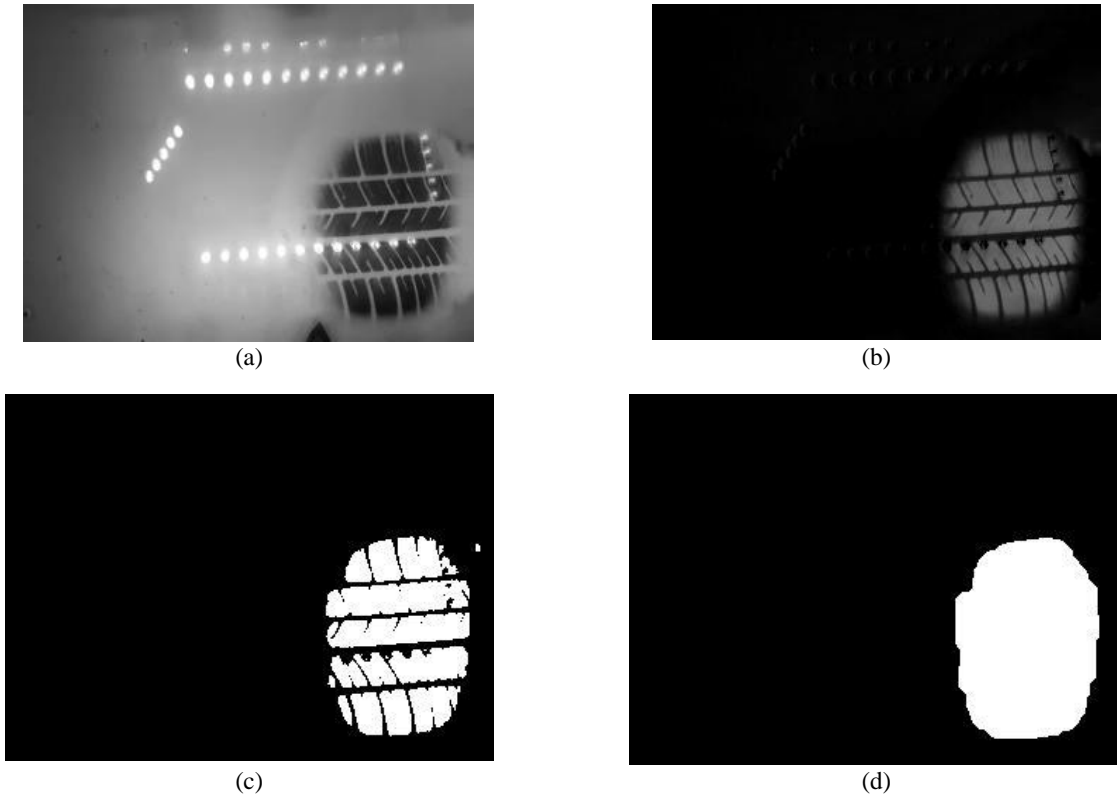


**Fig 3.** a) A sample image captured by the imaging system, b) the result of subtracting the background from current frame, c) the result of binarization stage, d) binary image after morphological filtering

The shape and size of contact patch depends on the tire inflation pressure and load on the tire. Fig 4 illustrates the shape of the contact patch for different values of load and tire inflation pressure. To measure the contact patch, the segmented image is scanned and the number of white pixels is counted. The contact patch in terms of  $\text{cm}^2$  is obtained by multiplication of the number of white pixels with a calibration factor, which is  $0.105^2$  in

our setup. The calibration factor is experimentally defined by counting the number of pixels corresponding to an object that its size is known. The contact area measured in this manner is called experimental contact patch (ECP) in the following sections of this paper. It is employed in Eq 10 to define a fitness function used by the Bat algorithm.

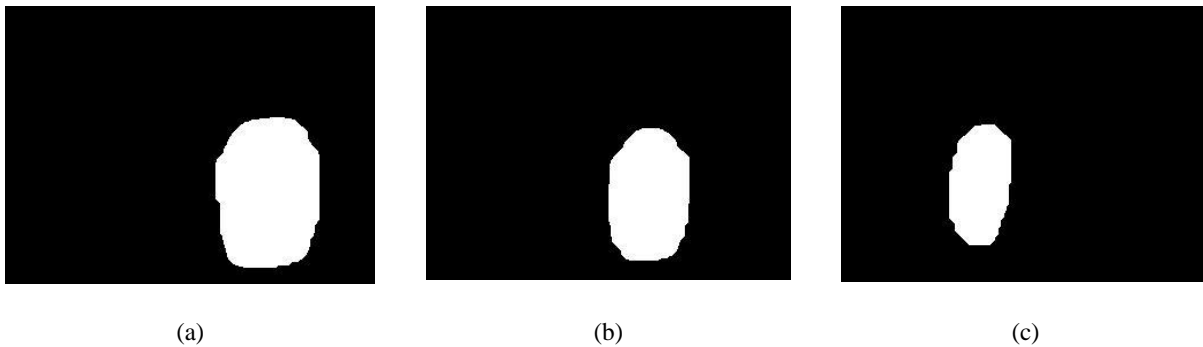


**Fig 4.** The shape and size of contact area for different values of load and inflation pressure, a)  $P_1W_5$ , b)  $P_2W_3$ , c)  $P_3W_1$

## A model for estimation of contact patch

The proposed imaging and processing system can be employed to measure the contact patch for different conditions. To develop an applicable model that can estimate the contact patch in operational condition without using the illustrated setup, the contact patch is calculated for some different conditions and bat algorithm is utilized for optimization purpose.

### Background of the bat algorithm

The bat algorithm is a powerful evolutionary optimization method, inspired by social behavior of bats and the phenomenon of echolocation to recognize distances. In this algorithm, each bat is defined by its position  $x_i^t$ , velocity  $v_i^t$ , frequency  $f_i$ , loudness  $A_i^t$ , and the emission pulse rate  $r_i^t$ . The positions of bats represent the solutions to the problem of interest (Wang & Guo, 2013). The velocity and position of each bat are updated according to Eqs 5-7, to find the best solution.

$$f_i = f_{\min} - (f_{\max} - f_{\min}) \times \beta \quad (5)$$

$$v_i^t = v_i^{t-1} + (x_i^{t-1} - x_*) f_i \quad (6)$$

$$x_i^t = x_i^{t-1} + v_i^t \quad (7)$$

Where  $x_*$  is the best solution found so far and  $\beta \in [0, 1]$  is a random value drawn from a uniform distribution.

The BA also includes a random walk search around the best solution by Eq 8:

$$x_{new} = x_{old} + \varepsilon A \quad (8)$$

Where  $\varepsilon$  is a random vector drawn from uniform distribution and  $A$  represents the average loudness of bats.

The basic steps of the bat algorithm (BA) can be described as shown in Algorithm 1 [15].

---

Algorithm 1: BAT algorithm

---

**Begin**

**Step 1: Initialization.** Set 1 the generation counter  $t = 1$ ; Initialize the population of  $N$  bats and their

---



---

Parameters randomly, where each bat corresponding to a potential solution of the given problem.

**Step 2: While** the termination criteria is not satisfied **or**  $t < \text{MaxGeneration}$  **do**

Generate new solutions by adjusting frequency, and updating velocities and locations/solutions [Eq 5–7]

**if** ( $\text{rand}() > r_i^t$ ) **then**

Select a solution among the best solutions;

Generate a local solution around the selected best solution using Eq (8)

**end if**

**if** ( $\text{rand}() < A_i^t$  &  $f(x_i) < f(x_*)$ ) **then**

Accept the new solution

Increase  $r_i$  and reduce  $A_i$

**end if**

Rank the bats and find the current best  $x_*$

$t = t + 1$ ;

**end while**

**Step 3:** Report the location of best bat as solution of problem.

**End.**

---

### Designing of the contact patch model

To develop the model, its general form is proposed based on our knowledge about the dependency of contact patch on the load and tire inflation pressure. It is apparent that increasing the load and decreasing the tire inflation pressure led to increase of contact patch. Therefore, the following equation can be an appropriate candidate model for the estimation of contact patch.

$$CP = \frac{k_1 W^{k_2}}{1 + k_3 P^{k_4}} \quad (9)$$

Where  $CP$  represents the contact patch model,  $W$  and  $P$  denote the load and tire inflation pressure values, respectively.  $k_1 - k_4$  are the model parameters, adjusted using bat algorithm. To find the best solution, the bat algorithm minimizes the cost function presented by Eq 10.

$$f(k_1, k_2, k_3, k_4) = \sum_{i=1}^I \sum_{j=1}^J \left( ECP(w_i, p_j) - \frac{k_1 w_i^{k_2}}{1 + k_3 p_j^{k_4}} \right)^2 \quad (10)$$

Where  $ECP(w_i, p_j)$  is the experimental contact patch measured by the proposed image processing system, where the values of load and tire inflation pressure are set to  $w_i$  and  $p_j$ , respectively.  $I$  and  $J$  denote the number of load and tire inflation pressure levels examined in our research. Optimizing the cost function by BA results  $k_1 = 1.35, k_2 = 0.39, k_3 = 5.49$  and  $k_4 = 0.68$  for the model parameters.

The presented model is true for the tire with specified specifications. However, this research can show an interesting approach from how to measure the contact patch dynamically to how it can be modeled for other types of tires.

## RESULTS AND DISCUSSION

In order to quantitative analysis, compilation results are presented in three category comprising statistical analysis, graphical analysis, and model evaluation.

The effect of variable parameters on the contact patch was examined by a simple linear regression analysis to recognize the relationship between the

change in inflation pressure and load on the tire. The analyzed data was arranged in the form of Table 1.

**Table 1.** The effect of inflation pressure and load on the contact patch changes

Predictors	R <sup>2</sup>	Df	Sig
Pressure	0.559	1	0.000
Load	0.254	1	0.012
Pressure and load	0.813	2	0.000

According to the 4<sup>th</sup> column of Table 1, the regression test is significant at the 95% level. The R<sup>2</sup> of the linear regression is 55.9% and 25.4% for tire inflation pressure and load on the tire respectively. Needless to say, the effect of tire inflation pressure is more important than load on the tire. Above all, the R<sup>2</sup> of the reciprocal effect (pressure and load) is 81.3% which can indicate both parameters together have a significant effect on the contact patch variations.

To evaluate the effect of tire inflation pressure and load on the tire on contact patch value, its amount was monitored as a function of both parameters in different values of them (Fig 5).

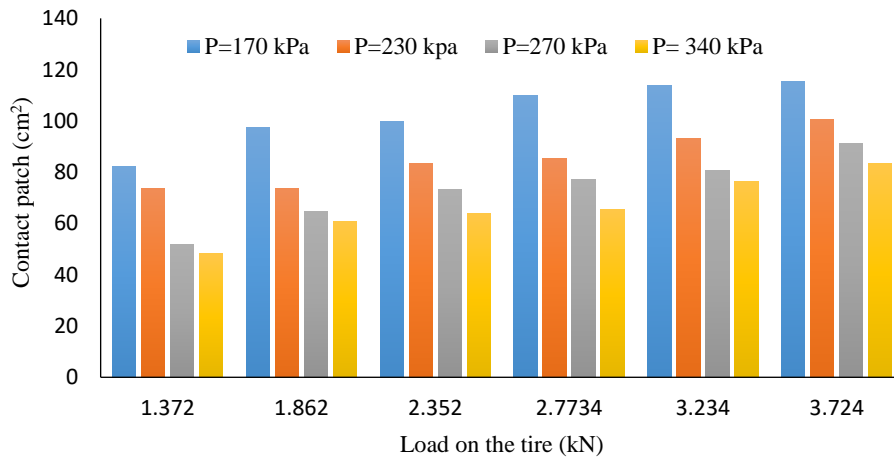


**Fig 5.** Tire contact patch values for different levels of inflation pressure and load on the tire

In the chart above, an increment in the amount of the contact patch can be observed in increasing the load on the tire, but the change at the greater load (3.724 kN) was small. Also at constant load, the tire contact patch is reduced with increasing tire inflation pressure, although, the rate of decrease in high pressure is lower.

The final model is obtained in terms of load and inflation pressure by optimizing the coefficients of Eq 9 as follows.

$$CP = \frac{1.35W^{0.39}}{1 + 5.49P^{0.68}} \quad (11)$$

To evaluate the model, three criteria were proposed comprising visual evaluation by graphical chart, MAPE determination and MSE.

In order to investigate the accuracy of the model in the graphic form, four charts (Fig 6 to Fig 9) were presented for the four variables (inflation pressure) involved in the experiment in terms of the load on the tire. In these charts, the abbreviations CPM and CPE stand for contact patch model and contact patch experimental respectively. As can be seen in these diagrams, there is a good match between the data obtained and the model data.

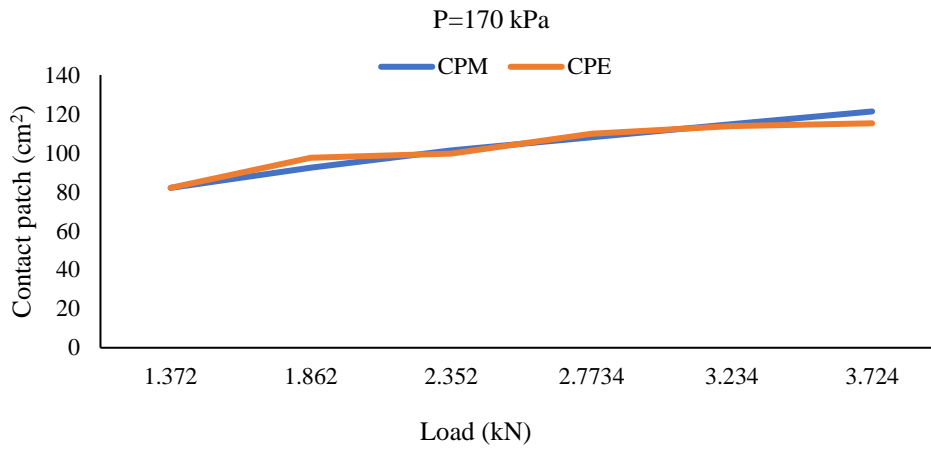


Fig 6. Visual evaluation of the proposed model in comparison with the actual values

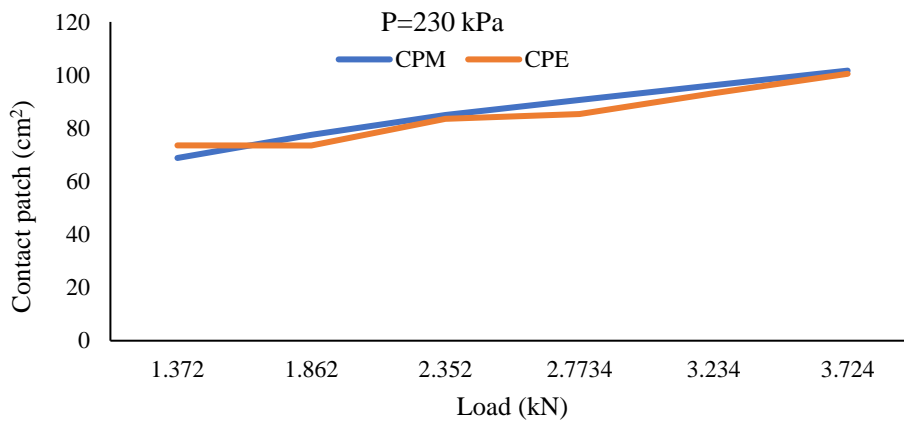
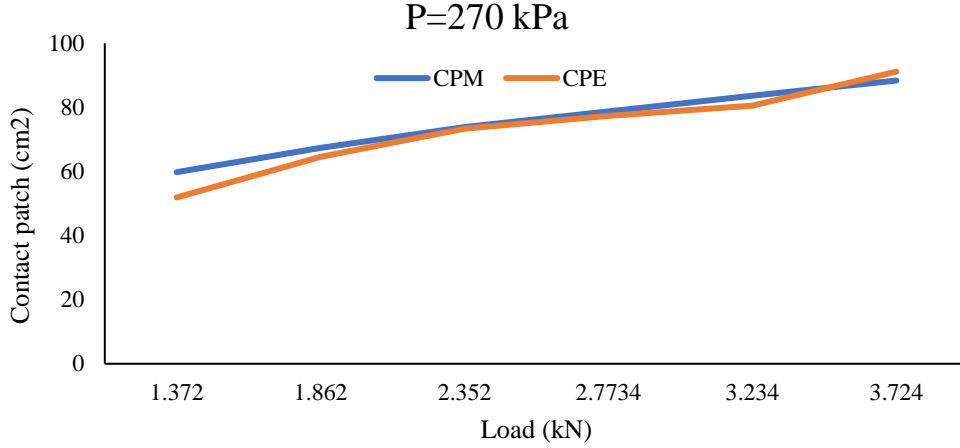
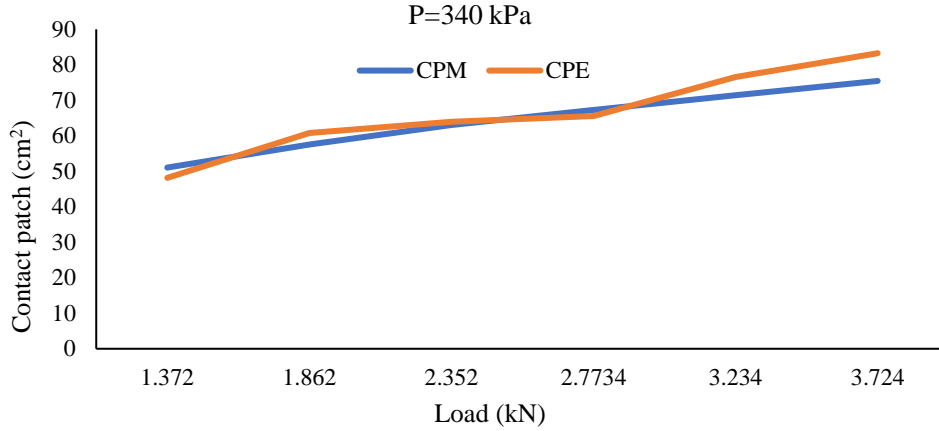


Fig 7. Visual evaluation of the proposed model in comparison with the actual values



**Fig 8.** Visual evaluation of the proposed model in comparison with the actual values



**Fig 9.** Visual evaluation of the proposed model in comparison with the actual values

In another analysis, The Mean Square Error (MSE) and the Mean Absolute Percentage Error (MAPE) (Prakash et al., 2019), obtained by utilizing following equations, were used as model evaluation criteria.

$$MSE = \frac{1}{N} \sum (CP_{Model} - CP_{Exp})^2 \quad (12)$$

$$MAPE = \frac{100}{N} \sum \frac{|CP_{Exp} - CP_{Model}|}{CP_{Exp}} \quad (13)$$

Based on the Eq 12 and Eq13, MSE and MAPE were calculated and reported to be associated with 14.51 and 4.14 % respectively. While the difference is being squaring in MSE, it can

describe different nuances about the prediction errors of model developed. However, MAPE discloses a clear interpretation of the model. In this case, the model developed has an error rate of about 4.14 % over experimental data. Coefficient of determination ( $R^2$ ) was another criterion used to assess the correlation between model and experimental data which is defined as the following equation.

$$R^2 = 1 - \frac{SS_{res}}{SS_{tot}} \quad (14)$$

Where  $SS_{res}$  and  $SS_{tot}$  are residual sum of squares and the total sum of squares respectively. Accordingly,  $R^2$  was achieved as 0.95, which

indicates a high correlation between the experimentally observed and predicted values. Most recent research has focused on how to measure this quantity, and dynamic models are rarely found. There was no similar research to compare our model with. However, in a research carried out in Texas Department of Transportation (Fernando et al., 2006), contact patch was modeled for six tires that the variable parameters were load and inflation pressure. The method of measuring the contact patch was statically which tire imprint was calculated for them. They reported  $R^2$  about 0.86 to 0.98 for six tires using multiple linear regression.

## CONCLUSION

Contact patch of the tire is considered as an important criterion in vehicle performance evaluation. Even the lateral forces, aligning torque of the tire and the fuel consumption of the vehicle are affected by this parameter. In most previous researches, the measurement of this parameter has been statically. Also, dynamic methods are limited to special laboratories. In this research, a novel method based on image processing techniques was utilized to measure contact patch while tire passes on the metal box and a model was estimated using the measured contact patches and BAT optimization algorithm. Evaluation of the model revealed that error rate compared with observed data (extracted from image processing) is equal to 4%. Moreover,  $R^2$  for this model was calculated as 95% which indicates the high credibility of the model for dynamic conditions.

## REFERENCES

- Abdi-pour, M., & Shamsi, M. (2023).** Design Methodology and Optimum Camera Setups for an Experimental Remote-Control Manipulator for Servicing Date Palms. *Biomechanism and Bioenergy Research*, 2(1), 76-83. <https://doi.org/10.22103/BBR.2023.20646.1038>
- Braghin, F., Brusarosco, M., Cheli, F., Cigada, A., Manzoni, S., & Mancosu, F. (2006).** Measurement of contact forces and patch features by means of accelerometers fixed inside the tire to improve future car active control. *Vehicle System Dynamics*, 44(sup1), 3-13. <https://doi.org/10.1080/00423110600867101>
- Derafshpour, S., Mardani, A., & Valizadeh, M. (2020).** Evolutionary algorithms application for improving the tire rolling resistance based on Wismer–Luth model. *Neural Computing and Applications*, 32, 5173-5183. <https://doi.org/10.1007/s00521-019-04012-3>
- Derafshpour, S., Valizadeh, M., Mardani, A., & Saray, M. T. (2019).** A novel system developed based on image processing techniques for dynamical measurement of tire-surface contact area. *Measurement*, 139, 270-276. <https://doi.org/10.1016/j.measurement.2019.02.074>
- Els, P., Stallmann, M., Botha, T., Guthrie, A., Wright, K., Augsburg, K., . . . Jimenez, E. (2016).** Comparison of tire footprint measurement techniques. International Design Engineering Technical Conferences and Computers and Information in Engineering Conference, <https://doi.org/10.1115/DETC2016-59944>
- Fernando, E. G., Musani, D., Park, D.-W., & Liu, W. (2006).** Evaluation of effects of tire size and inflation pressure on tire contact stresses and pavement response.
- Gillespie, T. (2021).** *Fundamentals of vehicle dynamics*. SAE international. <https://doi.org/10.4271/9781468601770>
- Godbole, R., Alcock, R., & Hettiaratchi, D. (1993).** The prediction of tractive performance on soil surfaces. *Journal of Terramechanics*, 30(6), 443-459. [https://doi.org/10.1016/0022-4898\(93\)90036-W](https://doi.org/10.1016/0022-4898(93)90036-W)
- Ivanov, V., & Augsburg, K. (2008).** Assessment of tire contact properties by nondestructive analysis. Part 1. The contact length in the region of adhesion at slow rolling velocities. *Journal of friction and wear*, 29, 362-368. <https://doi.org/10.3103/S1068366608050073>
- Kusaka, K., & Suzuki, T. (2013).** The statistical tire model and its application to vehicle dynamics design. *IFAC Proceedings Volumes*, 46(21), 77-82. <https://doi.org/10.3182/20130904-4-JP-2042.00024>

**Minca, C. (2015).** The determination and analysis of tire contact surface geometric parameters. *Review of the Air Force Academy*(1), 149.

**Prakash, C., Sujil, A., Kumar, R., & Mittal, N. (2019).** Linear prediction model for joint movement of lower extremity. Recent Findings in Intelligent Computing Techniques: Proceedings of the 5th ICACNI 2017, Volume 1, [https://doi.org/10.1007/978-981-10-8639-7\\_24](https://doi.org/10.1007/978-981-10-8639-7_24)

**Redrouthu, B. M., & Das, S. (2014).** Tyre modelling for rolling resistance.

**Rill, G. (2019).** Sophisticated but quite simple contact calculation for handling tire models. *Multibody System Dynamics*, 45(2), 131-153. <https://doi.org/10.1007/s11044-018-9629-4>

**Sreekumaran, A., & Iqbal, S. (2019).** *Thermal Mapping of HPAS System Based on Steering Kinematic and Tire-Road Contact Patch Sliding Model* (0148-7191). <https://doi.org/10.4271/2019-26-0225>

**Wang, G., & Guo, L. (2013).** A novel hybrid bat algorithm with harmony search for global numerical optimization. *Journal of Applied Mathematics*, 2013. <https://doi.org/10.1155/2013/696491>

**Zhang, Y., Yi, J., & Liu, T. (2013).** Embedded flexible force sensor for in-situ tire-road interaction measurements. *IEEE sensors Journal*, 13(5), 1756-1765. <https://doi.org/10.1109/JSEN.2013.2241051>